

文章编号:1009-9603(2019)05-0086-10

DOI:10.13673/j.cnki.cn37-1359/te.2019.05.011

## 非稳态窜流多段压裂水平井井底压力分析

姜瑞忠<sup>1</sup>,刘秀伟<sup>1</sup>,崔永正<sup>1</sup>,张春光<sup>1</sup>,郜益华<sup>2</sup>,潘红<sup>3</sup>,王星<sup>1</sup>

(1.中国石油大学(华东)石油工程学院,山东青岛266580; 2.中海油研究总院有限责任公司,北京100028; 3.中国石油大港油田分公司采油工艺研究院,天津300280)

**摘要:**多段压裂水平井技术是目前广泛应用于致密油开发的关键性技术。由于致密油储层基岩的孔喉为纳米级孔道且渗透率极低,所以不能忽略基岩中的非稳态窜流。为此建立了同时考虑启动压力梯度和应力敏感以及压裂改造区非稳态窜流的五线性流数学模型,通过Laplace变化、Pedrosa变化和扰动变化的方法求解数学模型,得到了拉式空间下的井底压力解,应用Stehfest数值反演的方法绘制双对数坐标下的压力动态曲线。研究表明,曲线可以分为6个流动阶段,且与现场实测数据拟合较好,从而验证了所建模型的合理性。同时对窜流系数、弹性储能比、主裂缝无因次渗透率模量、未改造区无因次启动压力梯度和渗透率进行敏感性参数分析,得出了各个敏感性参数对试井曲线形态的影响结果。

**关键词:**多段压裂水平井;非稳态窜流;启动压力梯度;应力敏感;影响因素分析;致密油

中图分类号:TE357.1

文献标识码:A

## Bottomhole pressure analysis of multistage fractured horizontal well during unsteady crossflow

JIANG Ruizhong<sup>1</sup>, LIU Xiuwei<sup>1</sup>, CUI Yongzheng<sup>1</sup>, ZHANG Chunguang<sup>1</sup>, GAO Yihua<sup>2</sup>, PAN Hong<sup>3</sup>, WANG Xing<sup>1</sup>

(1.School of Petroleum Engineering, China University of Petroleum(East China), Qingdao City, Shandong Province, 266580, China; 2.CNOOC Research Institute Co., Ltd., Beijing City, 100028, China; 3.Oil Production Technology Institute of Dagang Oilfield Company, CNPC, Tianjin City, 300280, China)

**Abstract:** Multistage fractured horizontal well is the one of the key techniques that has been widely used in the development of tight oil reservoirs at present. Because the pore throat of the tight oil reservoir is at nanoscale and the reservoir has extremely low permeability, the unsteady crossflow in the rock matrix cannot be ignored. Therefore, a five-linear flow mathematical model is proposed, in which the threshold pressure gradient, the stress sensitivity and the unsteady crossflow in unstimulated area are taken into account. Laplace transformation, Pedrosa's transformation and Perturbation transformation are applied to solve the mathematical model, and the bottomhole pressure at the Laplace Space is obtained, and the dynamic pressure curves are plotted in double logarithmic coordinates by Stehfest numerical inversion. The results show that the dynamic pressure curves can be divided into six flow stages and fit well with the field data, which verifies the model. Meanwhile, the crossflow coefficient, the elastic storativity ratio, the dimensionless permeability modulus of main fractures, the threshold pressure gradient, and the permeability of unstimulated reservoir are analyzed, so that the effects of these parameters on well testing curves are clarified.

**Key words:** multistage fractured horizontal well; unsteady crossflow; threshold pressure gradient; stress sensitivity; influencing factor analysis; tight oil

北美致密油的成功开采以及当今日益紧张的能源形势,使得非常规石油资源成为行业的热点<sup>[1-4]</sup>。由于致密油储层具有渗透率低、孔喉细小、流动条件差等特性<sup>[5-6]</sup>,导致常规水平井技术开发效

点<sup>[1-4]</sup>。由于致密油储层具有渗透率低、孔喉细小、流动条件差等特性<sup>[5-6]</sup>,导致常规水平井技术开发效

收稿日期:2019-04-25。

作者简介:姜瑞忠(1964—),男,江苏溧阳人,教授,博导,从事油气田开发与教学工作。联系电话:18678967281, E-mail: jrzhong@126.com。

基金项目:国家科技重大专项“低渗、特低渗油藏水驱扩大波及体积方法与关键技术”(2017ZX05013-002),国家自然科学基金项目“致密储层体积压裂缝网扩展模拟研究”(51574265)。

果不理想;而多段压裂水平井技术通过对水平井进行多段压裂形成多条裂缝通道,再加上水平井横向贯穿油层,能够大大提高油井产能,从而使得多段压裂水平井技术广泛应用于提高致密油产量<sup>[7]</sup>。对于多段压裂水平井的渗流规律,中外诸多学者对其进行了研究,其中使用最广泛的就是线性流模型。

BROWN等在2009年提出了三线性流模型研究多段压裂水平井的井底压力<sup>[8]</sup>,压力和压力导数在流动后期与MEDEIROS等提出的半解析解<sup>[9]</sup>拟合较好,验证了其模型的正确性;之后,姚军等在OZKAN模型基础上,建立了考虑启动压力梯度的三线性流模型,并研究启动压力梯度等因素的影响<sup>[10]</sup>,其压裂改造区采用Warrant-Root拟稳态窜流模型<sup>[11]</sup>。

2012年,STALGOROVA等建立五线性流多段压裂水平井模型与数值模型结果进行对比,验证了其模型的合理性<sup>[12]</sup>;之后,姬靖皓等建立了考虑启动压力梯度和应力敏感的五线性流模型<sup>[13]</sup>,其压裂改造区同样采用了Warrant-Root拟稳态窜流模型,绘制了相应的井底压力动态曲线;WU等采用等效渗透率将压裂改造区看作单重介质,同时综合考虑启动压力梯度和应力敏感建立了五线性流模型<sup>[14]</sup>。

但是由于致密油储层基岩孔喉为纳米级孔道,且渗透率极低,因此基岩中的非稳态窜流不能忽略<sup>[15]</sup>,应用Warrant-Root拟稳态窜流模型或者利用等效渗透率的方法所得到的解精确度不高。为此,笔者基于STALGOROVA五线性流模型,建立了同时存在启动压力梯度和应力敏感且考虑了压裂改造区之中非稳态窜流的不稳定渗流数学模型,并对其求解、绘制井底压力动态曲线。

### 1 物理模型

在对水平井实施多段压裂改造过程中,主裂缝周围多条天然裂缝会被连通从而形成复杂的缝网,但较远的储层并未受到压裂改造的影响,仍为致密储层(图1a)。依据其主裂缝和压裂改造区的分布特点,可简化得到其等效的流动模型(图1b)。由对称性可知,只需研究每条主裂缝控制区域的四分之一区域流动即可。将主裂缝控制区域的四分之一区域划分为5个区域(图2),区域1,2,3为未改造区域,看作单重介质;区域4为压裂改造区域,看作是双重介质,采用DE SWAAN模型<sup>[16]</sup>(图3);区域5为主裂缝区域。在区域1,2,3内考虑启动压力梯度的影响,区域4,5考虑应力敏感的影响。

物理模型基本假设为:①油藏的外边界为封闭

边界。②水平井位于油藏中心处且以定产量生产。③油藏中流体由未改造区流向改造区,再由改造区流向主裂缝,最后流向水平井。④地层岩石和流体微可压缩,流动过程温度不变,忽略重力、毛管压力以及井筒阻力的影响。

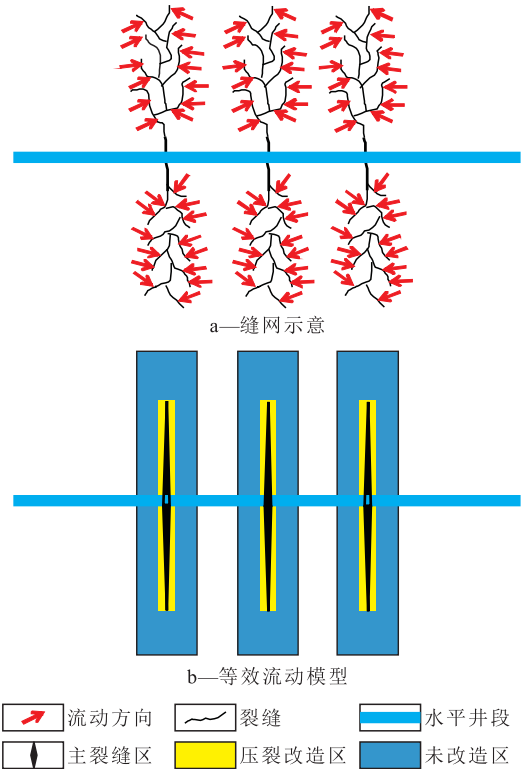


图1 多段压裂水平井物理模型  
Fig.1 Physical model for multistage fractured horizontal well

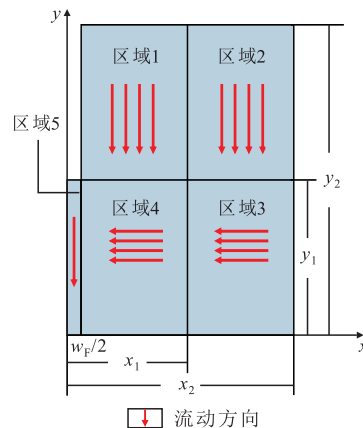


图2 主裂缝控制区域的四分之一区域流动方向示意  
Fig.2 Schematic of flow directions in a quarter area controlled by main fractures

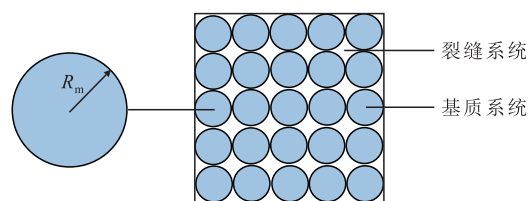


图3 裂缝与基质系统示意  
Fig.3 Schematic of fracture and matrix system

## 2 数学模型及求解

为方便推导与求解,定义无因次变量见表1。

表1 数学模型所包含的无因次变量  
Table1 Dimensionless variables contained in mathematical model

参数名称	表达式
无因次压力	$p_{jD} = \frac{nhK_{ref}}{1.842 \times 10^{-3} Q\mu B} (p_i - p_j) \quad j = 1, 2, 3, 4, 5$
无因次距离	$x_D = \frac{x}{L_{ref}}, y_D = \frac{y}{L_{ref}}, x_{1D} = \frac{x_1}{L_{ref}}, y_{1D} = \frac{y_1}{L_{ref}}, x_{2D} = \frac{x_2}{L_{ref}}, y_{2D} = \frac{y_2}{L_{ref}}$
无因次基质半径	$R_{mD} = \frac{R_m}{R_1}$
无因次主裂缝宽度	$w_D = \frac{w_F}{L_{ref}}$
无因次时间	$t_D = \frac{3.6\eta_{ref}}{L_{ref}^2} t \left( \eta_{ref} = \frac{K_{ref}}{\phi_{ref}\mu C_{ref}} \right)$
无因次导压系数	$\eta_{jD} = \frac{\eta_j}{\eta_{ref}} \quad j = 1, 2, 3, 4, 5$
无因次启动压力梯度	$G_{jD} = C_{vj} G_j L_{ref} \quad j = 1, 2, 3$
无因次渗透率模量	$\gamma_{jD} = \frac{1.842 \times 10^{-3} Q\mu B}{nhK_{ref}} \gamma_j \quad j = 4, 5$
窜流系数	$\lambda = 15 \frac{K_{4mi}}{K_{4fi}} \left( \frac{L_{ref}}{R_1} \right)^2$
弹性储容比	$\omega = \frac{\phi_{4fi} C_{i4f}}{\phi_{4fi} C_{i4f} + \phi_{4mi} C_{i4m}}$
无因次主裂缝导流能力	$F_{CD} = \frac{K_{5i} w_F}{K_{ref} L_{ref}}$

### 2.1 数学模型

#### 2.1.1 区域1

考虑启动压力梯度时区域1的渗流控制方程为:

$$\frac{\partial^2 p_1}{\partial y^2} - C_{11} G_1 \frac{\partial p_1}{\partial y} = \frac{\phi_{1i} \mu C_{i1}}{3.6K_{1i}} \times \frac{\partial p_1}{\partial t} \quad (1)$$

结合边界条件,对(1)式进行无因次化得到区域1无因次数学模型为:

$$\begin{cases} \frac{\partial^2 p_{1D}}{\partial y_D^2} - G_{1D} \frac{\partial p_{1D}}{\partial y_D} = \frac{1}{\eta_{1D}} \times \frac{\partial p_{1D}}{\partial t_D} \\ p_{1D} \Big|_{t_D=0} = 0 \\ \frac{\partial p_{1D}}{\partial y_D} \Big|_{y_D=y_{2D}} = 0 \\ p_{1D} \Big|_{y_D=y_{1D}} = p_{4D} \Big|_{y_D=y_{1D}} \end{cases} \quad (2)$$

#### 2.1.2 区域2

区域2与区域1同理可以得到考虑启动压力梯度时区域2的无因次数学模型为:

$$\begin{cases} \frac{\partial^2 p_{2D}}{\partial y_D^2} - G_{2D} \frac{\partial p_{2D}}{\partial y_D} = \frac{1}{\eta_{2D}} \times \frac{\partial p_{2D}}{\partial t_D} \\ p_{2D} \Big|_{t_D=0} = 0 \\ \frac{\partial p_{2D}}{\partial y_D} \Big|_{y_D=y_{2D}} = 0 \\ p_{2D} \Big|_{y_D=y_{1D}} = p_{3D} \Big|_{y_D=y_{1D}} \end{cases} \quad (3)$$

#### 2.1.3 区域3

由于区域2向区域3存在流体补充,可以将该流体补充项表示为:

$$q_{23} = \frac{1}{y_1} \times \frac{3.6K_{2i}}{\mu} \times \frac{\partial p_2}{\partial y} \Big|_{y=y_1} \quad (4)$$

从而推导得到区域3的渗流控制方程为:

$$\begin{aligned} \frac{\partial^2 p_3}{\partial x^2} - C_{13} G_3 \frac{\partial p_3}{\partial x} + \frac{1}{y_1} \times \frac{K_{2i}}{K_{1i}} \times \frac{\partial p_2}{\partial y} \Big|_{y=y_1} = \\ \frac{\phi_{3i} \mu C_{i3}}{3.6K_{3i}} \times \frac{\partial p_3}{\partial t} \end{aligned} \quad (5)$$

结合边界条件,对(5)式进行无因次化得到区域3无因次数学模型为:

$$\begin{cases} \frac{\partial^2 p_{3D}}{\partial x_D^2} - G_{3D} \frac{\partial p_{3D}}{\partial x_D} + \frac{1}{y_{1D}} \times \frac{K_{2i}}{K_{1i}} \times \frac{\partial p_{2D}}{\partial y_D} \Big|_{y_D=y_{1D}} = \\ \frac{1}{\eta_{3D}} \times \frac{\partial p_{3D}}{\partial t_D} \\ p_{3D} \Big|_{t_D=0} = 0 \\ \frac{\partial p_{3D}}{\partial x_D} \Big|_{x_D=x_{2D}} = 0 \\ p_{3D} \Big|_{x_D=x_{1D}} = p_{4D} \Big|_{x_D=x_{1D}} \end{cases} \quad (6)$$

#### 2.1.4 区域4

##### 2.1.4.1 基质系统

区域4基质的渗流控制方程为:

$$\frac{\partial^2 p_{4m}}{\partial R_m^2} + \frac{2}{R_m} \times \frac{\partial p_{4m}}{\partial R_m} = \frac{\phi_{4mi} \mu C_{i4m}}{3.6K_{4mi}} \times \frac{\partial p_{4m}}{\partial t} \quad (7)$$

结合边界条件,对(7)式无因次化后得到区域4基质系统无因次数学模型为:

$$\begin{cases} \frac{\partial^2 p_{4m}}{\partial R_{mD}^2} + \frac{2}{R_{mD}} \times \frac{\partial p_{4mD}}{\partial R_{mD}} = 15 \times \frac{1-\omega}{\lambda} \times \frac{1}{\eta_{4D}} \times \frac{\partial p_{4mD}}{\partial t_D} \\ p_{4mD} \Big|_{t_D=0} = 0 \\ p_{4mD} \Big|_{R_{mD}=1} = p_{4fD} \\ \frac{\partial p_{4mD}}{\partial R_{mD}} \Big|_{R_{mD}=0} = 0 \end{cases} \quad (8)$$

2.1.4.2 裂缝系统

区域4裂缝系统考虑到应力敏感效应,采用渗透率模量来表示裂缝渗透率为:

$$K_{4f} = K_{4fi} e^{-\gamma_4(p_i - p_{4f})} \quad (9)$$

同时,考虑到区域1向区域3的流体补充项以及基质与裂缝间的窜流项:

$$q_{14} = \frac{1}{y_1} \times \frac{3.6K_{li}}{\mu} \times \frac{\partial p_1}{\partial y} \Big|_{y=y_1} \quad (10)$$

$$q_m = -\frac{3}{R_1} \times \frac{3.6K_{mi}}{\mu} \times \frac{\partial p_{4m}}{\partial R_m} \Big|_{R_m=R_1} \quad (11)$$

可以推导得到区域4裂缝系统的渗流控制方程为:

$$\begin{aligned} e^{\gamma_4(p_{4f} - p_i)} \left[ \frac{\partial^2 p_{4f}}{\partial x^2} + \gamma_4 \left( \frac{\partial p_{4f}}{\partial x} \right)^2 \right] + \frac{K_{li}}{K_{4fi}} \times \frac{1}{y_1} \times \frac{\partial p_1}{\partial y} - \\ \frac{3}{R_1} \times \frac{K_{4mi}}{K_{4fi}} \times \frac{\partial p_{4m}}{\partial R_m} \Big|_{R_m=R_1} = \frac{\phi_{4fi} \mu C_{t4f}}{3.6K_{4fi}} \times \frac{\partial p_{4f}}{\partial t} \end{aligned} \quad (12)$$

结合边界条件,将(12)式无因次化后得到区域4裂缝系统无因次数学模型为:

$$\begin{cases} e^{-\gamma_{4D} p_{4fD}} \left[ \frac{\partial^2 p_{4fD}}{\partial x_D^2} - \gamma_{4D} \left( \frac{\partial p_{4fD}}{\partial x_D} \right)^2 \right] + \frac{1}{y_{1D}} \times \\ \frac{K_{li}}{K_{4fi}} \times \frac{\partial p_{1D}}{\partial y_D} \Big|_{y_D=y_{1D}} - \frac{\lambda}{5} \times \frac{\partial p_{4mD}}{\partial R_{mD}} \Big|_{R_{mD}=1} = \frac{\omega}{\eta_{4D}} \times \frac{\partial p_{4fD}}{\partial t_D} \\ p_{4fD} \Big|_{t_D=0} = 0 \\ K_{4fi} e^{-\gamma_{4D} p_{4fD}} \frac{\partial p_{4fD}}{\partial x_D} \Big|_{x_D=x_{1D}} = K_{3i} \frac{\partial p_{3D}}{\partial x_D} \Big|_{x_D=x_{1D}} \\ p_{4fD} \Big|_{x_D=\frac{w_D}{2}} = p_{5D} \Big|_{x_D=\frac{w_D}{2}} \end{cases} \quad (13)$$

2.1.5 区域5

和区域4裂缝系统相同,区域5同样考虑到应力敏感效应,渗透率受到压力影响,采用渗透率模

量来表示主裂缝渗透率为:

$$K_5 = K_{5i} e^{-\gamma_5(p_i - p_5)} \quad (14)$$

考虑到区域4向区域5的流体补充项:

$$q_{45} = \frac{2}{w_F} \times \frac{3.6K_{4fi} e^{\gamma_4(p_{4f} - p_i)}}{\mu} \times \frac{\partial p_{4f}}{\partial x} \Big|_{x=\frac{w_F}{2}} \quad (15)$$

可以推导得到区域5的渗流控制方程为:

$$\begin{aligned} e^{\gamma_5(p_5 - p_i)} \left[ \frac{\partial^2 p_5}{\partial y^2} + \gamma_5 \left( \frac{\partial p_5}{\partial y} \right)^2 \right] + \frac{2}{w_F} \times \frac{K_{4fi}}{K_{5i}} \times \\ e^{\gamma_4(p_{4f} - p_i)} \times \frac{\partial p_{4f}}{\partial x} \Big|_{x=\frac{w_F}{2}} = \frac{\phi_{5i} \mu C_{t5}}{3.6K_{5i}} \times \frac{\partial p_5}{\partial t} \end{aligned} \quad (16)$$

结合边界条件,将(16)式进行无因次化后可得到区域5无因次数学模型为:

$$\begin{cases} e^{-\gamma_{5D} p_{5D}} \left[ \frac{\partial^2 p_{5D}}{\partial y_D^2} - \gamma_{5D} \left( \frac{\partial p_{5D}}{\partial y_D} \right)^2 \right] + \frac{2}{w_D} \times \frac{K_{4fi}}{K_{5i}} \times \\ e^{-\gamma_{4D} p_{4fD}} \times \frac{\partial p_{4fD}}{\partial x_D} \Big|_{x_D=\frac{w_D}{2}} = \frac{1}{\eta_{5D}} \times \frac{\partial p_{5D}}{\partial t_D} \\ p_{5D} \Big|_{t_D=0} = 0 \\ \frac{\partial p_{5D}}{\partial y_D} \Big|_{y_D=y_{1D}} = 0 \\ e^{-\gamma_{5D} p_{5D}} \frac{\partial p_{5D}}{\partial y_D} \Big|_{y_D=0} = -\frac{\pi}{F_{CD}} \end{cases} \quad (17)$$

2.2 数学模型求解

2.2.1 区域1

将区域1无因次数学模型进行Laplace变化,得:

$$\begin{cases} \frac{\partial^2 \overline{p}_{1D}}{\partial y_D^2} - G_{1D} \frac{\partial \overline{p}_{1D}}{\partial y_D} = \frac{u}{\eta_{1D}} \overline{p}_{1D} \\ \frac{\partial \overline{p}_{1D}}{\partial y_D} \Big|_{y_D=y_{2D}} = 0 \\ \overline{p}_{1D} \Big|_{y_D=y_{1D}} = \overline{p}_{4fD} \Big|_{y_D=y_{1D}} \end{cases} \quad (18)$$

对(18)式偏微分方程进行求解可得:

$$\overline{p}_{1D} = \overline{p}_{4fD} \Big|_{y_D=y_{1D}} \frac{A_2 e^{A_1(y_D - y_{2D})} - A_1 e^{A_2(y_D - y_{2D})}}{A_2 e^{A_1(y_{1D} - y_{2D})} - A_1 e^{A_2(y_{1D} - y_{2D})}} \quad (19)$$

其中:

$$A_1 = \frac{G_{1D} + \sqrt{G_{1D}^2 + \frac{4u}{\eta_{1D}}}}{2} \quad (20)$$

$$A_2 = \frac{G_{1D} - \sqrt{G_{1D}^2 + \frac{4u}{\eta_{1D}}}}{2} \quad (21)$$

由于区域4的流动与x方向无关,故(19)式又可写为:

$$\frac{\overline{p_{1D}}}{\overline{p_{4D}}} = \frac{A_2 e^{A_1(y_D - y_{2D})} - A_1 e^{A_2(y_D - y_{2D})}}{A_2 e^{A_1(y_{1D} - y_{2D})} - A_1 e^{A_2(y_{1D} - y_{2D})}} \quad (22)$$

### 2.2.2 区域2

同理区域1求解方法,可以得到区域2的解为:

$$\frac{\overline{p_{2D}}}{\overline{p_{3D}}} = \frac{B_2 e^{B_1(y_D - y_{2D})} - B_1 e^{B_2(y_D - y_{2D})}}{B_2 e^{B_1(y_{1D} - y_{2D})} - B_1 e^{B_2(y_{1D} - y_{2D})}} \quad (23)$$

其中:

$$B_1 = \frac{G_{2D} + \sqrt{G_{2D}^2 + \frac{4u}{\eta_{2D}}}}{2} \quad (24)$$

$$B_2 = \frac{G_{2D} - \sqrt{G_{2D}^2 + \frac{4u}{\eta_{2D}}}}{2} \quad (25)$$

### 2.2.3 区域3

同理将区域3无因次数学模型进行Laplace变化,可得:

$$\begin{cases} \frac{\partial^2 \overline{p_{3D}}}{\partial x_D^2} - G_{3D} \frac{\partial \overline{p_{3D}}}{\partial x_D} + \frac{1}{y_{1D}} \times \frac{K_{2i}}{K_{3i}} \times \frac{\partial \overline{p_{2D}}}{\partial y_D} \Big|_{y_D = y_{1D}} = \frac{u}{\eta_{3D}} \overline{p_{3D}} \\ \frac{\partial \overline{p_{3D}}}{\partial x_D} \Big|_{x_D = x_{2D}} = 0 \\ \overline{p_{3D}} \Big|_{x_D = x_{1D}} = \overline{p_{4D}} \Big|_{x_D = x_{1D}} \end{cases} \quad (26)$$

由区域2压力解可得:

$$\frac{\partial \overline{p_{2D}}}{\partial y_D} \Big|_{y_D = y_{1D}} = \beta_2 \overline{p_{3D}} \quad (27)$$

其中:

$$\beta_2 = \frac{B_2 B_1 e^{B_1(y_{1D} - y_{2D})} - B_2 B_1 e^{B_2(y_{1D} - y_{2D})}}{B_2 e^{B_1(y_{1D} - y_{2D})} - B_1 e^{B_2(y_{1D} - y_{2D})}} \quad (28)$$

将(27)式代入(26)式得:

$$\begin{cases} \frac{\partial^2 \overline{p_{3D}}}{\partial x_D^2} - G_{3D} \frac{\partial \overline{p_{3D}}}{\partial x_D} - f_3(u) \overline{p_{3D}} = 0 \\ \frac{\partial \overline{p_{3D}}}{\partial x_D} \Big|_{x_D = x_{2D}} = 0 \\ \overline{p_{3D}} \Big|_{x_D = x_{1D}} = \overline{p_{4D}} \Big|_{x_D = x_{1D}} \end{cases} \quad (29)$$

其中:

$$f_3(u) = \frac{u}{\eta_{3D}} - \frac{K_{2i}}{K_{3i}} \beta_2 \quad (30)$$

对(29)式进行求解得区域3压力解为:

$$\overline{p_{3D}} = \overline{p_{4D}} \Big|_{x_D = x_{1D}} \frac{C_2 e^{C_1(x_D - x_{2D})} - C_1 e^{C_2(x_D - x_{2D})}}{C_2 e^{C_1(x_{1D} - x_{2D})} - C_1 e^{C_2(x_{1D} - x_{2D})}} \quad (31)$$

其中:

$$C_1 = \frac{G_{3D} + \sqrt{G_{3D}^2 + 4f_3(u)}}{2} \quad (32)$$

$$C_2 = \frac{G_{3D} - \sqrt{G_{3D}^2 + 4f_3(u)}}{2} \quad (33)$$

### 2.2.4 区域4

#### 2.2.4.1 基质系统

将区域4基质系统无因次数学模型进行Laplace变化可得:

$$\begin{cases} \frac{1}{R_{mD}^2} \times \frac{\partial}{\partial R_{mD}} \left( R_{mD}^2 \frac{\partial \overline{p_{4mD}}}{\partial R_{mD}} \right) = 15 \times \frac{1 - \omega}{\lambda} \times \frac{u}{\eta_{4D}} \times \overline{p_{4mD}} \\ \overline{p_{4mD}} \Big|_{R_{mD} = 1} = \overline{p_{4D}} \\ \frac{\partial \overline{p_{4mD}}}{\partial R_{mD}} \Big|_{R_{mD} = 0} = 0 \end{cases} \quad (34)$$

对(34)式求解可得:

$$\overline{p_{mD}} = \frac{\overline{p_{4D}}}{R_{mD}} \times \frac{\sinh(R_{mD} D)}{\sinh D} \quad (35)$$

其中:

$$D = \sqrt{\frac{1 - \omega}{\lambda} \times \frac{u}{\eta_{4D}}} \quad (36)$$

#### 2.2.4.2 裂缝系统

由于(13)式中无因次渗透率模量的存在,使得该数学模型具有很强的非线性,为了便于求解,此利用Pedrosa<sup>[17]</sup>变化以及摄动变化式消除非线性,其计算式为:

$$p_{4mD}(x_D, t_D) = -\frac{1}{\gamma_{4D}} \ln \left[ 1 - \gamma_{4D} \tau_4(x_D, t_D) \right] \quad (37)$$

$$\tau_4 = \tau_{40} + \gamma_{4D} \tau_{41} + \gamma_{4D}^2 \tau_{42} + \dots \quad (38)$$

$$\frac{1}{1 - \gamma_{4D} \tau_4} = 1 + \gamma_{4D} \tau_4 + (\gamma_{4D} \tau_4)^2 + \dots \quad (39)$$

由于 $\gamma_{4D}$ 为小量,所以零阶摄动解 $\tau_{40}$ 可以看作是近似解且具有足够的精度要求,故对区域4裂缝系统数学模型进行Pedrosa变化以及摄动变化,然后进行Laplace变化得:

$$\left\{ \begin{aligned} \left. \frac{\partial^2 \bar{\tau}_{40}}{\partial x_D^2} + \frac{1}{y_{1D}} \times \frac{K_{1i}}{K_{4fi}} \times \frac{\partial \bar{p}_{1D}}{\partial y_D} \right|_{y_D=y_{1D}} - \frac{1}{5} \lambda \left. \frac{\partial \bar{p}_{mD}}{\partial R_{mD}} \right|_{R_{mD}=1} &= \frac{\omega}{\eta_{4D}} u \bar{\tau}_{40} \\ \left. K_{4fi} \frac{\partial \bar{\tau}_{40}}{\partial x_D} \right|_{x_D=x_{1D}} &= \left. K_{3i} \frac{\partial \bar{p}_{3D}}{\partial x_D} \right|_{x_D=x_{1D}} \\ \left. \bar{\tau}_{40} \right|_{x_D=\frac{w_D}{2}} &= \left. \bar{\tau}_{50} \right|_{x_D=\frac{w_D}{2}} \end{aligned} \right. \quad (40)$$

由区域1压力解可得:

$$\left. \frac{\partial \bar{p}_{1D}}{\partial y_D} \right|_{y_D=y_{1D}} = \beta_1 \bar{p}_{4fD} \approx \beta_1 \bar{\tau}_{40} \quad (41)$$

其中:

$$\beta_1 = \frac{A_2 A_1 e^{A_1(y_{1D}-y_{2D})} - A_2 A_1 e^{A_2(y_{1D}-y_{2D})}}{A_2 e^{A_1(y_{1D}-y_{2D})} - A_1 e^{A_2(y_{1D}-y_{2D})}} \quad (42)$$

由区域4基质系统压力解可得:

$$\left. \frac{\partial \bar{p}_{mD}}{\partial R_{mD}} \right|_{R_{mD}=1} = \beta_m \bar{p}_{4fD} \approx \beta_m \bar{\tau}_{40} \quad (43)$$

其中:

$$\beta_m = D \times \coth D - 1 \quad (44)$$

由区域3压力解可得:

$$\left. \frac{\partial \bar{p}_{3D}}{\partial x_D} \right|_{x_D=x_{1D}} = \beta_3 \bar{p}_{4fD} \Big|_{x_D=x_{1D}} \approx \beta_3 \bar{\tau}_{40} \Big|_{x_D=x_{1D}} \quad (45)$$

其中:

$$\beta_3 = \frac{C_2 C_1 e^{C_1(x_{1D}-x_{2D})} - C_2 C_1 e^{C_2(x_{1D}-x_{2D})}}{C_2 e^{C_1(x_{1D}-x_{2D})} - C_1 e^{C_2(x_{1D}-x_{2D})}} \quad (46)$$

将(41)式、(43)式和(45)式代入(40)式可得:

$$\left\{ \begin{aligned} \frac{\partial^2 \bar{\tau}_{40}}{\partial x_D^2} - f_4(u) \bar{\tau}_{40} &= 0 \\ \left. K_{4fi} \frac{\partial \bar{\tau}_{40}}{\partial x_D} \right|_{x_D=x_{1D}} &= \left. K_{3i} \frac{\partial \bar{p}_{3D}}{\partial x_D} \right|_{x_D=x_{1D}} \\ \left. \bar{\tau}_{40} \right|_{x_D=\frac{w_D}{2}} &= \left. \bar{\tau}_{50} \right|_{x_D=\frac{w_D}{2}} \end{aligned} \right. \quad (47)$$

其中:

$$f_4(u) = \frac{\omega}{\eta_{4D}} u - \frac{1}{y_{1D}} \times \frac{K_{1i}}{K_{4fi}} \beta_1 + \frac{1}{5} \lambda \beta_m \quad (48)$$

对(47)式进行求解得到:

$$\bar{\tau}_{40} = \bar{\tau}_{50} \times \frac{\left( E_2 - \frac{K_{3i}}{K_{4fi}} \beta_3 \right) e^{E_1 \left( x_D - x_{1D} \right)} - \left( E_1 - \frac{K_{3i}}{K_{4fi}} \beta_3 \right) e^{E_2 \left( x_D - x_{1D} \right)}}{\left( E_2 - \frac{K_{3i}}{K_{4fi}} \beta_3 \right) e^{E_1 \left( \frac{w_D}{2} - x_{1D} \right)} - \left( E_1 - \frac{K_{3i}}{K_{4fi}} \beta_3 \right) e^{E_2 \left( \frac{w_D}{2} - x_{1D} \right)}} \quad (49)$$

其中:

$$E_1 = \sqrt{f_4(u)} \quad (50)$$

$$E_2 = -\sqrt{f_4(u)} \quad (51)$$

### 2.2.5 区域5

区域5主裂缝数学模型求解与区域4裂缝系统数学模型求解相同,利用Pedrosa变化以及摄动变化消除非线性,然后进行Laplace变化可得:

$$\left\{ \begin{aligned} \frac{\partial^2 \bar{\tau}_{50}}{\partial y_D^2} + \frac{2}{w_D} \times \frac{K_{4fi}}{K_{5i}} \times \frac{\partial \bar{\tau}_{40}}{\partial x_D} \Big|_{x_D=\frac{w_D}{2}} &= \frac{u}{\eta_{5D}} \bar{\tau}_{50} \\ \left. \frac{\partial \bar{\tau}_{50}}{\partial y_D} \right|_{y_D=y_{1D}} &= 0 \\ \left. \frac{\partial \bar{\tau}_{50}}{\partial y_D} \right|_{y_D=0} &= -\frac{\pi}{F_{CD} u} \end{aligned} \right. \quad (52)$$

由区域4压力解得:

$$\left. \frac{\partial \bar{\tau}_{40}}{\partial x_D} \right|_{x_D=\frac{w_D}{2}} = \beta_4 \bar{\tau}_{50} \quad (53)$$

其中:

$$\beta_4 = \frac{\left( E_2 - \frac{K_{3i}}{K_{4fi}} \beta_3 \right) E_1 e^{E_1 \left( \frac{w_D}{2} - x_{1D} \right)} - \left( E_1 - \frac{K_{3i}}{K_{4fi}} \beta_3 \right) E_2 e^{E_2 \left( \frac{w_D}{2} - x_{1D} \right)}}{\left( E_2 - \frac{K_{3i}}{K_{4fi}} \beta_3 \right) e^{E_1 \left( \frac{w_D}{2} - x_{1D} \right)} - \left( E_1 - \frac{K_{3i}}{K_{4fi}} \beta_3 \right) e^{E_2 \left( \frac{w_D}{2} - x_{1D} \right)}} \quad (54)$$

将(53)式代入(52)式可得:

$$\left\{ \begin{aligned} \frac{\partial^2 \bar{\tau}_{50}}{\partial y_D^2} - f_5(u) \bar{\tau}_{50} &= 0 \\ \left. \frac{\partial \bar{\tau}_{50}}{\partial y_D} \right|_{y_D=y_{1D}} &= 0 \\ \left. \frac{\partial \bar{\tau}_{50}}{\partial y_D} \right|_{y_D=0} &= -\frac{\pi}{F_{CD} u} \end{aligned} \right. \quad (55)$$

其中:

$$f_5(u) = \frac{u}{\eta_{5D}} - \frac{2}{w_D} \times \frac{K_{4fi}}{K_{5i}} \beta_4 \quad (56)$$

对(55)式进行求解可得:

$$\overline{\tau}_{50} = \frac{\pi}{F_{CD}} \times \frac{1}{\sqrt{f_5(u)}} \times \frac{\cosh[(y_D - y_{1D})\sqrt{f_5(u)}]}{\sinh[y_{1D}\sqrt{f_5(u)}]} \quad (57)$$

当 $y_D = 0$ 时,主裂缝压力解即为Laplace空间下无因次井底压力解为:

$$\overline{p_{wD0}} = \overline{\tau}_{50} \Big|_{y_D=0} = \frac{\pi}{F_{CD}} \times \frac{1}{\sqrt{f_5(u)}} \times \coth[y_{1D}\sqrt{f_5(u)}] \quad (58)$$

同时采用Duhamel原理引入无因次井筒储集系数和表皮系数,得到考虑井筒储集效应和表皮效应的井底压力解为:

$$\overline{p_{wD}} = \frac{\overline{p_{wD0}} + S}{u[1 + C_D u(\overline{p_{wD0}} + S)]} \quad (59)$$

对(59)式进行Stehfest数值反演<sup>[18]</sup>,然后进行摄动反变化,便可得到真实空间下的井底压力解为:

$$p_{wD} = -\frac{\ln[1 - \gamma_{5D} L^{-1}(p_{wD})]}{\gamma_{5D}} \quad (60)$$

### 3 井底压力曲线形态分析

依据前面推导出的真实空间下的无因次井底压力解,在双对数坐标系下绘制无因次井底压力曲线和无因次井底压力导数曲线,据此来描述渗流过程。

#### 3.1 流动形态划分

由双对数坐标系下的无因次井底压力和无因次井底压力导数曲线(图4)可见,流动形态可以划分为6个阶段:①早期井筒储集效应阶段,无因次井底压力和无因次井底压力导数曲线重合且逐渐上升。②表皮效应阶段,井筒储集效应减弱,无因次井底压力和无因次井底压力导数曲线开始分离,且无因次井底压力导数曲线达到一定值后开始下降,形成明显的驼峰,而无因次井底压力曲线则继续上升。③压裂改造区基质与裂缝的非稳态窜流阶段,无因次井底压力导数曲线呈现出一个“凹子”形状,无因次井底压力曲线继续上升。④整个压裂改造区的线性流阶段,无因次井底压力和无因次井底压力导数曲线上升。⑤压裂改造区和未改造区的线性流阶段,无因次井底压力和无因次井底压力导数曲线继续上升并且逐渐接近。⑥受边界影响的流

动阶段,无因次井底压力和无因次井底压力导数曲线最终再次重合,且继续上升。

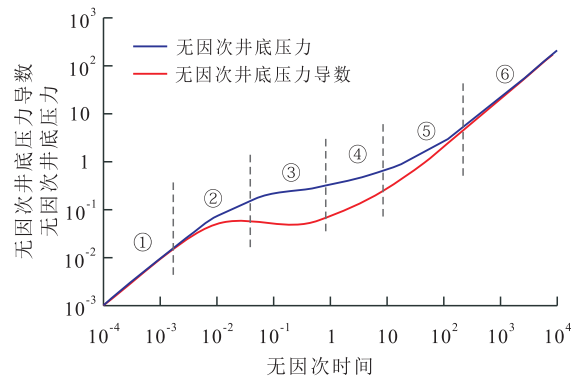


图4 多段压裂水平井井底压力动态曲线

Fig.4 Dynamic curve of bottomhole pressure in multistage fractured horizontal well

#### 3.2 模型验证与对比

松辽盆地致密油藏X区块某井在实施多段压裂增产措施一段时间后进行了压力恢复试井测试,现场实测数据为时间-压力关系,进行模型验证时,将实测数据进行无因次化,然后绘制实测数据的双对数压力特征曲线,并与所建立的五线性流压力特征曲线进行对比。从图5可以看到,早期井筒储集效应阶段的数据点并未测出,但是中间区域的数据点与五线性流压力特征曲线拟合较好,呈现出较为明显的2个线性流阶段,且具有窜流的“凹子”特征,从而验证了所建模型的合理性。

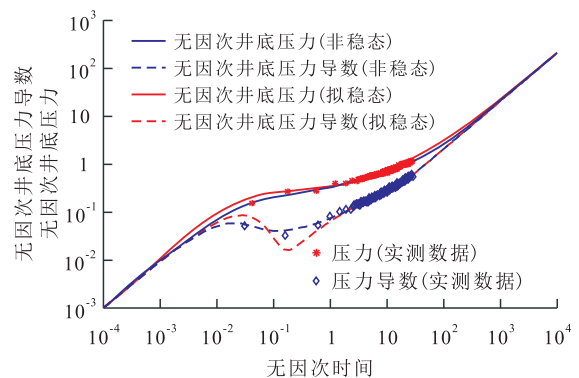


图5 模型验证与对比

Fig.5 Model verification and comparison

从图5也可以看到,与考虑拟稳态窜流的试井曲线相对比,在前期和后期两者曲线基本一致。而在窜流阶段,非稳态窜流无因次井底压力导数曲线上的窜流“凹子”要比拟稳态的浅且宽。其原因为所取的计算参数相同时,非稳态窜流条件下基质系统中的流体对系统压力改变的响应要比拟稳态条件下更敏感<sup>[19]</sup>,因此不会像拟稳态一样出现很明显的“凹子”段,且无因次井底压力和无因次井底压力导数曲线上对于窜流阶段的反映会更早。

### 3.3 参数敏感性分析

#### 3.3.1 窜流系数

从图6可以看出,随着窜流系数的增加,无因次井底压力曲线逐渐下移,无因次井底压力导数曲线上非稳态窜流的“凹子”相应前移,窜流发生的时间变早。其原因为,窜流系数越大,表明基质系统渗透率与裂缝系统渗透率差别越小,基质与裂缝之间的窜流在较小的压差下就可以发生,裂缝中的压力达到基质向裂缝窜流的压力条件所需时间较短,进而“凹子”前移,窜流发生变早。

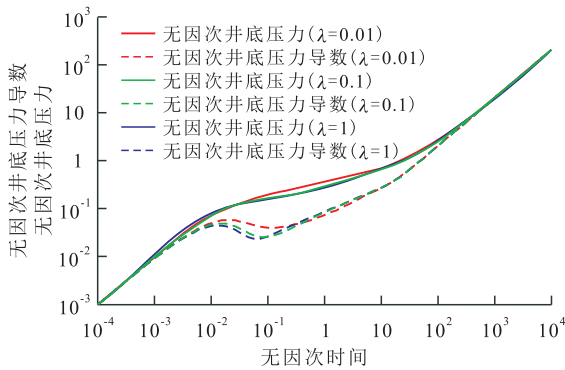


图6 窜流系数对压力动态曲线的影响

Fig.6 Effect of crossflow coefficient on dynamic pressure curve

#### 3.3.2 弹性储容比

从图7可以看出,随着弹性储容比的减小,无因次井底压力导数曲线的非稳态窜流“凹子”略变宽变深,并没有拟稳态窜流时变化那么明显。其原因为,弹性储容比越小,裂缝储集的流体越少,裂缝供液能力弱,开井生产短时间内裂缝系统会产生较大压降,而基质系统向裂缝系统的流体补充需要较长时间才可以使得裂缝系统压力提升,从而使得“凹子”略变宽变深。

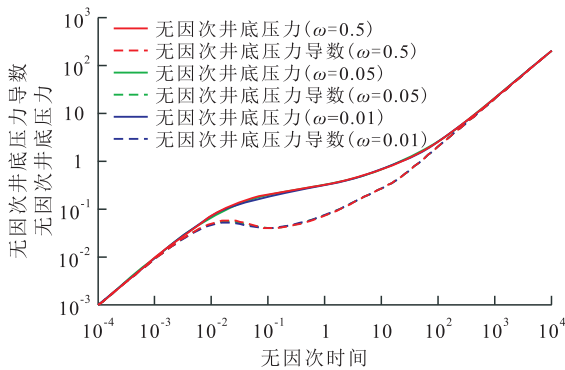


图7 弹性储容比对压力动态曲线的影响

Fig.7 Effect of elastic storativity ratio on dynamic pressure curve

#### 3.3.3 主裂缝渗透率模量

从图8可以看出,随主裂缝无因次渗透率模量的增加,无因次井底压力和无因次井底压力导数曲

线主要在边界控制流阶段发生变化,无因次井底压力和无因次井底压力导数曲线随之上翘。其原因为,在流动阶段初期,整个生产过程中压降相对较小,地层压力变化较小,此时主裂缝渗透率受压力的影响较小,应力敏感性弱,但一段时间后,地层压力变化较大,主裂缝渗透率应力敏感性增强,且无因次渗透率模量越大,渗透率变化越大,渗流阻力越大,流体流动所需的压差越大,从而造成压力和压力导数曲线的上翘。

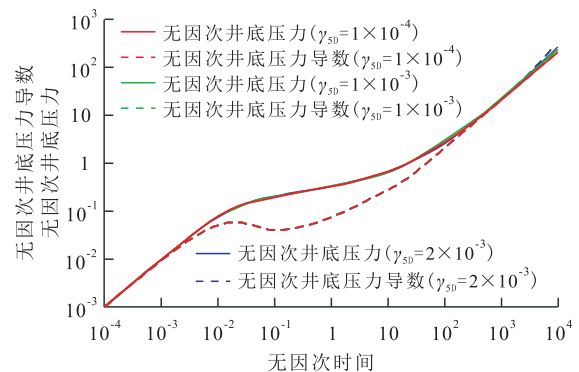


图8 主裂缝渗透率模量对压力动态曲线的影响

Fig.8 Effect of permeability modulus of main fractures on dynamic pressure curve

#### 3.3.4 未改造区域启动压力梯度和渗透率

从图9可以看出,未改造区域的无因次启动压力梯度取值的增加造成无因次井底压力和无因次井底压力导数曲线的上移。因无因次启动压力梯度的增加,未改造区域物性变差,流体流动阻力变大,压力消耗越大,导致无因次井底压力和无因次井底压力导数曲线下移。

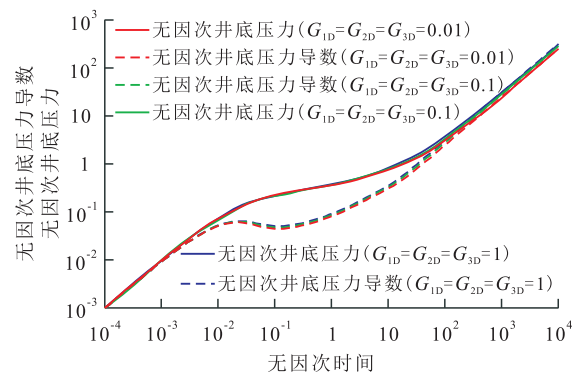


图9 未改造区域启动压力梯度对压力动态曲线的影响

Fig.9 Effect of threshold pressure gradient in unstimulated area on pressure dynamic curve

未改造区域渗透率的增加则会造成无因次井底压力和无因次井底压力导数曲线的下移,与无因次启动压力梯度正好相反(图10)。因渗透率的增加,未改造区域物性变好,渗流阻力减小,压力消耗较小,导致无因次井底压力和无因次井底压力导数



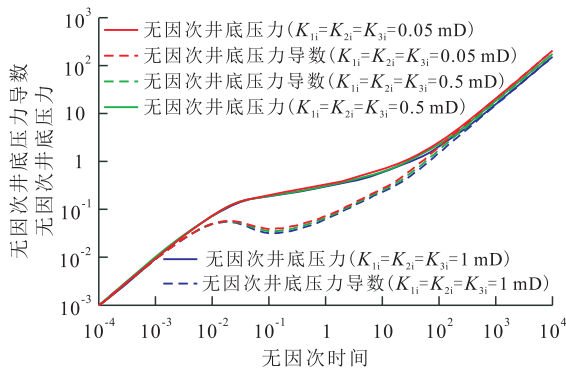


图10 未改造区域渗透率对压力动态曲线的影响

Fig.10 Effect of permeability of unstimulated area on dynamic pressure curve

曲线下移。

## 4 结论

为了多段压裂水平井开发提供理论依据,建立了考虑压裂改造区非稳态窜流的五线性流数学模型,通过Laplace变化、Pedrosa变化以及摄动变化等一系列数学物理方法,求出解析解。依据流动形态,将试井曲线分为6个阶段:早期井筒储集效应阶段、表皮效应阶段、压裂改造区基质与裂缝的非稳态窜流阶段、整个压裂改造区的线性流阶段、压裂改造区和未改造区的线性流阶段以及受边界影响的流动阶段。

依据数学模型的敏感性参数分析认为:窜流系数越大,非稳态窜流出现得越早;弹性储容比的减小,会造成无因次井底压力导数曲线上的“凹子”变宽变深,但并不明显;随着主裂缝无因次渗透率模量的增大,边界控制流阶段的无因次井底压力和无因次井底压力导数曲线上翘;未改造区域的无因次启动压力梯度的增加会造成未改造区域物性变差,无因次井底压力和无因次井底压力导数曲线上移;相反,未改造区域渗透率的增加则会造成未改造区域物性变好,无因次井底压力和无因次井底压力导数曲线下移。

### 符号解释

$x, y$ ——距离, m;  $w_f$ ——主裂缝宽度, m;  $x_1$ ——压裂改造区半宽, m;  $x_2$ ——主裂缝半间距, m;  $y_1$ ——裂缝半长, m;  $y_2$ ——油藏半宽, m;  $R_m$ ——基质系统圆形球体的球向半径, m;  $p_{jD}$ ——第  $j$  区无因次压力;  $j$ ——区域编号, 其值为 1—5;  $n$ ——主裂缝数目;  $h$ ——油藏厚度, m;  $K_{ref}$ ——参考渗透率, mD;  $Q$ ——单条主裂缝产量,  $m^3/d$ ;  $\mu$ ——地层原油黏度, mPa·s;  $B$ ——原油体积系数;  $p$ ——压力, MPa;  $i$ ——初始值;  $x_D$ ,

$y_D$ ——无因次距离;  $L_{ref}$ ——参考长度, m;  $x_{1D}$ ——无因次压裂改造区半宽;  $y_{1D}$ ——无因次裂缝半长;  $x_{2D}$ ——无因次主裂缝半间距;  $y_{2D}$ ——无因次油藏半宽;  $R_{mD}$ ——基质系统圆形球体的无因次球向半径;  $R_1$ ——基质系统圆形球体颗粒半径, m;  $w_D$ ——无因次主裂缝宽度;  $t_D$ ——无因次时间;  $\eta_{ref}$ ——参考导压系数,  $\mu m^2/(mPa \cdot s \cdot MPa^{-1})$ ;  $t$ ——时间, h;  $\phi_{ref}$ ——参考孔隙度;  $C_{ref}$ ——参考综合压缩系数,  $MPa^{-1}$ ;  $\eta_{jD}$ ——第  $j$  区无因次导压系数;  $\eta_j$ ——第  $j$  区导压系数,  $\mu m^2/(mPa \cdot s \cdot MPa^{-1})$ ;  $G_{jD}$ ——第  $j$  区无因次启动压力梯度;  $C_{jD}$ ——第  $j$  区流体压缩系数,  $MPa^{-1}$ ;  $G_j$ ——第  $j$  区启动压力梯度,  $MPa/m$ ;  $\gamma_{jD}$ ——第  $j$  区无因次渗透率模量;  $\gamma_j$ ——第  $j$  区渗透率模量,  $MPa^{-1}$ ;  $\lambda$ ——窜流系数;  $K_{4mi}$ ——区域 4 基质系统初始渗透率, mD;  $K_{4fi}$ ——区域 4 裂缝系统初始渗透率, mD;  $\omega$ ——弹性储容比;  $\phi_{4fi}$ ——区域 4 裂缝系统初始孔隙度;  $C_{4fi}$ ——区域 4 裂缝系统综合压缩系数,  $MPa^{-1}$ ;  $\phi_{4mi}$ ——区域 4 基质系统初始孔隙度;  $C_{4mi}$ ——区域 4 基质系统综合压缩系数,  $MPa^{-1}$ ;  $F_{CD}$ ——裂缝导流能力;  $K_{5i}$ ——区域 5 初始渗透率, mD;  $p_1$ ——区域 1 压力, MPa;  $C_{1i}$ ——区域 1 流体压缩系数,  $MPa^{-1}$ ;  $G_1$ ——区域 1 启动压力梯度,  $MPa/m$ ;  $\phi_{1i}$ ——区域 1 初始孔隙度;  $C_{1i}$ ——区域 1 综合压缩系数,  $MPa^{-1}$ ;  $K_{1i}$ ——区域 1 初始渗透率, mD;  $p_{1D}$ ——区域 1 无因次压力;  $G_{1D}$ ——区域 1 无因次启动压力梯度;  $\eta_{1D}$ ——区域 1 无因次导压系数;  $p_{4D}$ ——区域 4 裂缝系统无因次压力;  $p_{2D}$ ——区域 2 无因次压力;  $G_{2D}$ ——区域 2 无因次启动压力梯度;  $\eta_{2D}$ ——区域 2 无因次导压系数;  $p_{3D}$ ——区域 3 无因次压力;  $q_{23}$ ——区域 2 向区域 3 的流体补充项;  $K_{2i}$ ——区域 2 的初始渗透率, mD;  $p_2$ ——区域 2 压力, MPa;  $p_3$ ——区域 3 压力, MPa;  $C_{13}$ ——区域 3 流体压缩系数,  $MPa^{-1}$ ;  $G_3$ ——区域 3 启动压力梯度,  $MPa/m$ ;  $\phi_{3i}$ ——区域 3 初始孔隙度;  $C_{13}$ ——区域 3 综合压缩系数,  $MPa^{-1}$ ;  $K_{3i}$ ——区域 3 初始渗透率, mD;  $G_{3D}$ ——区域 3 无因次启动压力梯度;  $\eta_{3D}$ ——区域 3 无因次导压系数;  $p_{4m}$ ——区域 4 基质系统压力, MPa;  $p_{4mD}$ ——区域 4 基质系统无因次压力;  $\eta_{4D}$ ——区域 4 无因次导压系数;  $K_{4f}$ ——区域 4 裂缝系统渗透率, mD;  $\gamma_4$ ——区域 4 裂缝系统渗透率模量,  $MPa^{-1}$ ;  $p_i$ ——初始压力, MPa;  $p_{4f}$ ——区域 4 裂缝系统压力, MPa;  $q_{14}$ ——区域 1 向区域 4 的流体补充项;  $q_m$ ——区域 4 基质系统与裂缝系统间的窜流项;  $K_{4mi}$ ——区域 4 基质系统渗透率, mD;  $\gamma_{4D}$ ——区域 4 裂缝系统无因次渗透率模量;  $K_5$ ——区域 5 渗透率, mD;  $\gamma_5$ ——区域 5 渗透率模量,  $MPa^{-1}$ ;  $p_5$ ——区域 5 压力, MPa;  $q_{45}$ ——区域 4 向区域 5 的流体补充项;  $\phi_{5i}$ ——区域 5 初始孔隙度;  $C_{15}$ ——区域 5 综合压缩系数,  $MPa^{-1}$ ;  $p_{5D}$ ——区域 5 无因次压力;  $\eta_{5D}$ ——区域 5 无因次导压系数;  $u$ ——Laplace 因子;  $\gamma_{4D}$ ——区域 4 裂缝系统无因次渗透率模量;  $A_1, A_2, B_1, B_2, C_1, C_2, D, E_1, E_2, \beta_1, \beta_2, \beta_3, \beta_4, \beta_m, f_3(u), f_4(u), f_5(u)$ ——中间变量;  $\tau_{40}, \tau_{50}$ ——摄动变化后的区域 4 和区域 5 无因次压力;  $p_{wD0}$ ——未考虑井筒储集和表皮系数的无因次井底压力;  $p_{wD}$ ——考虑井筒储集和表皮系数的无因次井底压力;

$S$ ——表皮系数; $C_D$ ——无因次井筒储集系数。

### 参考文献

- [1] 庞正炼,邹才能,陶士振,等.中国致密油形成分布与资源潜力评价[J].中国工程科学,2012,14(7):60-67.  
PANG Zhenglian, ZOU Caineng, TAO Shizhen, et al. Formation, distribution and resource evaluation of tight oil in China[J]. Engineering Science, 2012, 14(7): 60-67.
- [2] 林森虎,邹才能,袁选俊,等.美国致密油开发现状及启示[J].岩性油气藏,2011,23(4):25-30,64.  
LIN Senhu, ZOU Caineng, YUAN Xuanjun, et al. Status quo of tight oil exploitation in the United States and its implication[J]. Lithologic Reservoirs, 2011, 23(4): 25-30, 64.
- [3] 许怀先,李建忠.致密油——全球非常规石油勘探开发新热点[J].石油勘探与开发,2012,39(1):99.  
XU Huaixian, LI Jianzhong. Tight oil: A new hot spot for unconventional oil exploration and development in the world[J]. Petroleum Exploration and Development, 2012, 39(1): 99.
- [4] 张抗.从致密油气到页岩油气——中国非常规油气发展之路探析[J].中国地质教育,2012,21(2):9-15.  
ZHANG Kang. From tight oil & gas to shale oil & gas—Approach for the development of unconventional oil & gas in China[J]. Chinese Geological Education, 2012, 21(2): 9-15.
- [5] 贾承造,邹才能,李建忠.中国致密油评价标准、主要类型、基本特征及资源前景[J].石油学报,2012,33(3):343-350.  
JIA Chengzao, ZOU Caineng, LI Jianzhong. Assessment criteria, main types, basic features and resource prospects of the tight oil in China[J]. Acta Petrolei Sinica, 2012, 33(3): 343-350.
- [6] 吴颜雄,薛建勤,杨智,等.柴西地区扎哈泉致密油储层特征及评价[J].世界地质,2018,37(4):167-176.  
WU Yanxiong, XUE Jianqin, YANG Zhi, et al. Characteristics and evaluation of tight oil reservoirs in Zhahaquan area, western Qaidam Basin[J]. Global Geology, 2018, 37(4): 167-176.
- [7] 虞婷婷.分段压裂水平井线性流模型适用条件研究[D].成都:西南石油大学,2016.  
YU Tingting. Study on the applicable conditions of linear flow model for multi-stage fractured horizontal wells [D]. Chengdu: Southwest Petroleum University, 2016.
- [8] BROWN Margaret, OZKAN Erdal, RAGHAVAN Rajagopal, et al. Practical solutions for pressure transient responses of fractured horizontal wells in unconventional reservoirs [R]. SPE 125043, 2009: 1-18.
- [9] MEDEIROS F, OZKAN E, KAZEMI H. Productivity and drainage area of fractured horizontal wells in tight gas reservoirs [R]. SPE 108110, 2008: 902-911.
- [10] 姚军,殷修杏,樊冬艳,等.低渗透油藏的压裂水平井三线性流测试井模型[J].油气井测试,2011,20(5):1-5.  
YAO Jun, YIN Xiuxing, FAN Dongyan, et al. Trilinear-flow well test model of fractured horizontal well in low permeability reservoir [J]. Well Testing, 2011, 20(5): 1-5.
- [11] WARREN J E, ROOT P J. The behavior of naturally fractured reservoirs [J]. SPE Journal, 1963, 3(3): 245-255.
- [12] STALGOROVA E, MATTAR L. Analytical model for history matching and forecasting production in multistage fractured horizontal wells [C]. Calgary: SPE Canadian Unconventional Resources Conference, 2012.
- [13] 姬靖皓,姚约东,马雄强,等.致密油藏体积压裂水平井不稳定压力分析[J].水动力学研究与进展: A辑,2017,32(4):491-501.  
JI Jinghao, YAO Yuedong, MA Xiongqiang, et al. Pressure transient analysis for volume-fractured horizontal well in tight oil reservoirs [J]. Journal of Hydrodynamics: Series A, 2017, 32(4): 491-501.
- [14] WU Zhongwei, CUI Chuazhi, LÜ Guangzhong, et al. A multi-linear transient pressure model for multistage fractured horizontal well in tight oil reservoirs with considering threshold pressure gradient and stress sensitivity [J]. Journal of Petroleum Science and Engineering, 2018, 172: 839-854.
- [15] 彭凯,宁正福,王桂丽.页岩气藏双重介质渗流模型研究[J].重庆科技学院学报:自然科学版,2012,14(1):8-11,22.  
PENG Kai, NING Zhengfu, WANG Guili, et al. Study for flow model in dual-porosity of shale gas reservoirs [J]. Journal of Chongqing University of Science and Technology: Natural Science Edition, 2012, 14(1): 8-11, 22.
- [16] DE SWAAN O A. Analytic solutions for determining naturally fractured reservoir properties by well testing [J]. Society of Petroleum Engineers Journal, 1976, 16(3): 117-122.
- [17] PEDROSA O A. Pressure transient response in stress sensitive formations [C]. Oakland: SPE California Regional Meeting, 1986.
- [18] 同登科,陈钦雷.关于Laplace数值反演Stehfest方法的一点注记[J].石油学报,2001,22(6):91-92.  
TONG Dengke, CHEN Qinlei. A note on the Laplace numerical inversion Stehfest method [J]. Acta Petrolei Sinica, 2011, 22(6): 91-92.
- [19] 高杰.页岩气藏多段压裂水平井压力动态特征研究[D].成都:西南石油大学,2014.  
GAO Jie. Study on dynamic pressure characteristics of multi-stage fractured horizontal well in shale gas reservoir [D]. Chengdu: Southwest Petroleum University, 2014.

编辑 王星